

Challenges for Reinforcement Learning in Quantum Circuit Design

Philipp Altmann¹ Jonas Stein¹ Michael Kölle¹ Adelina Bärligea² Thomas Gabor¹ Thomy Phan³
Sebastian Feld⁴ Claudia Linnhoff-Popien¹

Abstract

Quantum computing (QC) in the current NISQ era is still limited in size and precision. Hybrid applications mitigating those shortcomings are prevalent to gain early insight and advantages. Hybrid quantum machine learning (QML) comprises both the application of QC to improve machine learning (ML) and ML to improve QC architectures. This work considers the latter, leveraging reinforcement learning (RL) to improve the search for viable quantum architectures, which we formalize by a set of generic challenges. Furthermore, we propose a concrete framework, formalized as a Markov decision process, to enable learning policies capable of controlling a universal set of continuously parameterized quantum gates. Finally, we provide benchmark comparisons to assess the shortcomings and strengths of current state-of-the-art RL algorithms.

1. Introduction

Quantum circuits comprise a combination of unitary compositions, or quantum gates, executed on a quantum computer to alter a certain quantum state. Mostly driven by theoretical promises of achieving exponential speed-ups in computational tasks such as integer factorization (Shor, 1999) and solving linear equation systems (Harrow et al., 2009), quantum computing (QC) has become a rapidly growing field of research. However, the current era of *noisy intermediate-scale quantum* (NISQ) hardware (Preskill, 2018) poses considerable limitations that prevent the realization of these speed-ups. Moreover, prevalent circuit architectures are mostly hand-crafted. The central task of *quantum circuit design* therefore consists of finding a sequence of quantum gates to achieve a certain objective, potentially given (hardware) limitations. We mainly consider two categories,

¹LMU Munich, Germany ²TU Munich, Germany ³University of Southern California, USA ⁴Delft University of Technology Delft, The Netherlands. Correspondence to: Philipp Altmann <philipp.altmann@ifi.lmu.de>.

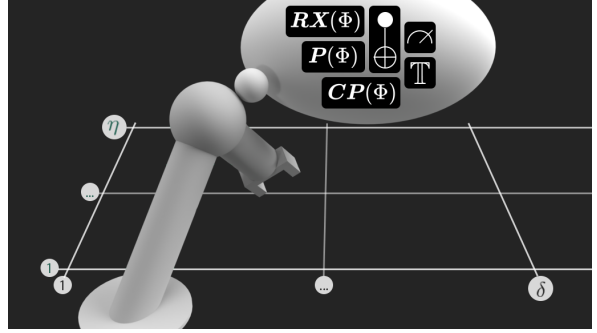


Figure 1. *Quantum Circuit Designer* for η qubits with depth δ

architecture search and circuit optimization, more specifically, the preparation of arbitrary states and the composition of unitary operations.

Among other ML approaches, we find *reinforcement learning* (RL) to be specifically suited for these objectives, learning tasks in various discrete and continuous sequential decision-making problems, without the need for granular specification, with temporal dependence. Also, sophisticated mechanisms balancing exploration and exploitation provide a helpful foundation to discover viable architectures. Through this research, our aim is to provide comprehensive insight into various objectives associated with quantum circuit design, and thereby to foster collaboration and innovation within the AI research community. However, in contrast to most related work, we approach this topic bottom-up by dividing problems of interest into their core objectives, aiming to shed light on challenges that current RL algorithms face in this field of research. Overall, we provide the following contributions:

- We formulate core objectives for reinforcement learning arising from quantum circuit design (QCD).
- We define a generic RL framework for QCD to learn executing parameterized operations (cf. Fig. 1).
- We demonstrate challenges that current state-of-the-art RL approaches face in QCD.

2. Background

Quantum Computing First, we provide a brief overview of the basic concepts of quantum computing. For more detailed information, see [Nielsen & Chuang \(2010\)](#). A quantum computer is built from qubits (wires) to execute a quantum circuit defined by a sequence of elementary operations (quantum gates) to carry and manipulate the quantum state. Unlike classical bits, which can be in the state 0 or 1, qubits can take on any superposition of these two, so that their state can be represented as:

$$\alpha |0\rangle + \beta |1\rangle = \alpha \begin{bmatrix} 1 \\ 0 \end{bmatrix} + \beta \begin{bmatrix} 0 \\ 1 \end{bmatrix} = \begin{bmatrix} \alpha \\ \beta \end{bmatrix} \in \mathbb{C}^2. \quad (1)$$

$|0\rangle$ and $|1\rangle$ are quantum computational basis states of the two-dimensional Hilbert space spanned by one qubit, and $|\alpha|^2 + |\beta|^2 = 1$. A two-qubit state can be represented by $|ab\rangle = |a\rangle |b\rangle = |a\rangle \otimes |b\rangle \in \mathbb{C}^{2^2}$, with the 2^2 computational basis states $|00\rangle, |01\rangle, |10\rangle$, and $|11\rangle$. Following this formulation, quantum gates can be understood as unitary matrix operations $U \in \mathbb{C}^{2^n \times 2^n}$ applied to the state vector of the n qubits, on which the gate acts. Their only condition of being unitary (i.e., $UU^\dagger = I$) ensures that the operations inherent in them are reversible. With the identity I , the most elementary single-gate operations contain:

$$I = \begin{bmatrix} 1 & 0 \\ 0 & 1 \end{bmatrix}; \quad X = \begin{bmatrix} 0 & 1 \\ 1 & 0 \end{bmatrix}; \quad Z = \begin{bmatrix} 1 & 0 \\ 0 & -1 \end{bmatrix}. \quad (2)$$

To represent arbitrary quantum operations also requires two-qubit gates, such as the well-known CNOT gate, which is the quantum version of the classical XOR gate:

$$CX_{a,b} = |0\rangle\langle 0| \otimes I + |1\rangle\langle 1| \otimes X \quad (3)$$

A CNOT gate flips the state of the target qubit $|b\rangle$ if and only if the control qubit $|a\rangle = |1\rangle$. In fact, it can be shown that any multi-qubit logic gate (i.e., unitary matrix of arbitrary size) can be composed of CNOT and single-qubit gates, which is a concept called *universality* of gate sets ([Barenco et al., 1995](#)). One universal set of gates, close to current quantum hardware, consists of CNOT (3), X-Rotation (4), and PhaseShift (5) operations ([Kitaev, 1997](#)):

$$RX(\lambda) = \exp\left(-i\frac{\lambda}{2}X\right) \quad (4)$$

$$P(\phi) = \exp\left(i\frac{\phi}{2}\right) \cdot \exp\left(-i\frac{\phi}{2}Z\right) \quad (5)$$

In addition, we use the *Controlled-PhaseShift* defined as:

$$CP(\phi) = I \otimes |0\rangle\langle 0| + P(\phi) \otimes |1\rangle\langle 1| \quad (6)$$

Furthermore we refer to the gate set $\{CX, H, S\}$ as the *Clifford group*, representing an alternative universal gate set with $S = P(\pi/2)$, and the Hadamard operator H :

$$H = \frac{1}{\sqrt{2}} \begin{bmatrix} 1 & 1 \\ 1 & -1 \end{bmatrix} \quad (7)$$

Reinforcement Learning We formulate our problem of quantum circuit design as a *Markov decision process (MDP)* $M = \langle \mathcal{S}, \mathcal{A}, \mathcal{P}, \mathcal{R}, \gamma \rangle$ with discrete time steps t , a set \mathcal{S} of states s_t , a set \mathcal{A} of actions a_t , the transition probability $\mathcal{P}(s_{t+1} | s_t, a_t)$ from s_t to s_{t+1} when executing a_t , a scalar reward $r_t = \mathcal{R}(s_t, a_t)$, and the discount factor $\gamma \in [0, 1)$ for calculating the *discounted return* $G_t = \sum_{k=0}^{\infty} \gamma^{t+k} r_{t+k}$ ([Puterman, 2014](#)). The goal is to find an optimal *policy* π^* with the action-selection probability $\pi(a_t | s_t)$ that maximizes the expected return. Policy π can be evaluated with the *value function* $Q^\pi(s_t, a_t) = \mathbb{E}_\pi[G_t | s_t, a_t]$ or the *state-value function* $V^\pi(s_t) = \mathbb{E}_{\pi, \mathcal{P}}[G_t | s_t]$. The *optimal value function* $Q^* = Q^{\pi^*}$ of any *optimal policy* π^* satisfies $Q^* \geq Q^{\pi'}$ for all policies π' and state-action pairs $\langle s_t, a_t \rangle \in \mathcal{S} \times \mathcal{A}$.

Value-based RL approaches such as DQN approximate the optimal value function Q^* using parameterized function approximators Q_θ to derive a behavior policy π based on multiarmed bandit selection ([Watkins & Dayan, 1992](#); [Mnih et al., 2015](#)). Alternatively, *Policy-based RL* approximates π^* from trajectories τ of experience tuples $\langle s_t, a_t, r_t, s_{t+1} \rangle$ generated by π_θ , directly learning the policy parameters θ via gradient ascent on $\nabla_\theta \mathbb{E}_{\pi_\theta}[G(\tau)]$ ([Watkins & Dayan, 1992](#); [Sutton & Barto, 2018](#)). For simplicity, we omit the parameter indices θ of π , V , and Q for the following. *Advantage Actor-Critic (A2C)* incorporates the value network V^π to build the advantage $A_t^\pi = Q^\pi(s_t, a_t) - V^\pi(s_t)$, enabling updates using policy rollouts of incomplete episodes, where π represents the actor and V^π represents the critic ([Mnih et al., 2016](#)). *Proximal Policy Optimization (PPO)* offers an alternative approach, maximizing the surrogate objective $L = \min\{\omega_t A_t^\pi, \text{clip}(\omega_t, 1 - \epsilon, 1 + \epsilon) A_t^\pi\}$, with $\omega_t = \frac{\pi(a_t | s_t)}{\pi_{old}(a_t | s_t)}$, where $\pi_{old}(a_t | s_t)$ is the previous policy, and the clipping parameter ϵ restricts the magnitude of policy updates ([Schulman et al., 2017](#)). PPO has been recently proven to ensure stable policy improvement, thus being a theoretically sound alternative to vanilla actor-critic approaches ([Grudzien et al., 2022](#)). Similarly, applying clipping to twin Q functions in combination with delayed policy updates with *Twin Delayed DDPG (TD3)*, has been shown to improve *Deep Deterministic Policy Gradient (DDPG)*, approximating both Q and π ([Dankwa & Zheng, 2019](#)). Building upon those improvements, *Soft Actor Critic (SAC)* bridges the gap between value-based Q-learning and policy gradient approaches and has shown state-of-the-art performance in various continuous control robotic benchmark tasks ([Haarnoja et al., 2018](#)).

Yet, most RL algorithms face central challenges like exploring sparse reward landscapes and high-dimensional (continuous) action spaces. Nevertheless, besides robotic control or image-based games, RL has already been successfully applied to a wide range of current challenges in QC ([Bukov et al., 2018](#); [Colomer et al., 2020](#); [van der Linde et al., 2023](#)).

3. Related Work

In the following, we survey said challenges in quantum architecture search and circuit optimization.

Quantum Architecture Search Currently, prevailing circuit architectures are predominantly designed manually for specific purposes, such as the *variational quantum eigensolver* (VQE) (Peruzzo et al., 2014). *Quantum architecture search* (QAS) denotes the process of automatically engineering quantum circuits to find a sequence of quantum gates achieving a certain task (Zhang et al., 2022). Specifically, we consider the composition of unitaries (UC), the preparation of a quantum state (SP), and the simulation of a given Hamiltonian (HS) (Bharti et al., 2022).

While evolutionary algorithms are commonly used for their efficiency in searching large problem spaces, they often produce problem-specific circuits (Rattew et al., 2019; Chivilikhin et al., 2020). In contrast, motivated by the sequential nature of quantum circuits, we approach QAS as a decision-making problem. Similarly, Ostaszewski et al. (2021) propose using RL to generate VQE Hamiltonians. However, their work denotes a problem-specific top-down approach, whereas we strive for a bottom-up approach, formulating generic RL challenges from the field of QAS. Likewise, RL has been proposed to prepare certain states (Kuo et al., 2021; Sogabe et al., 2022), producing a more generic challenge. Similar to Sogabe et al. (2022), we propose a reward based on the distance between the final and target states, where Kuo et al. (2021) use a distance threshold, introducing an additional hyperparameter. The decomposition of a given unitary operation using RL constitutes an additional challenge (Zhang et al., 2020; Pirhooshyaran & Terlaky, 2021). Note that we propose the inverse challenge of composing a target unitary rather than performing a backward search starting from the target state. Yet, composing a valid operation that does not only apply to a specific input state, but also to all possible inputs, requires even more precision.

Overall, to the best of our knowledge, existing approaches only utilize discrete gate sets, such as the Clifford group defined above (Kölle et al., 2024). Using operations with predefined parameterizations might require a two-step procedure of first generating a circuit architecture and then optimizing the circuit parameterization. Traditionally, classical optimization routines are employed to perform this task, including gradient-free approaches, such as evolutionary algorithms, and gradient-based approaches using the parameter-shift rule (Crooks, 2019). Note that both methods require numerous circuit executions to find optimal parameters. In contrast, our approach seeks to integrate this parameter optimization task directly into the RL environment, by enabling continuous actions. Thus, agents inherently seek optimal parameters in the generated circuits.

Quantum Circuit Optimization In addition to searching for feasible circuit architectures, RL has also been considered for *quantum circuit optimization* (QCO). The most apparent challenge in QCO is optimizing the circuit structure itself to globally reduce its depth and gate count. From a given quantum circuit, the goal is to find a logically equivalent circuit using fewer gates, thus reducing the runtime. In addition to approaches such as the use of ZX calculus (Kissinger & van de Wetering, 2020), employing RL has also been proposed, either, with the agent operating on the entire circuit (Fösel et al., 2021), or, incorporating optimization through a gate-by-gate procedure (Ostaszewski et al., 2021). Ostaszewski et al. (2021) even argue that RL will naturally find shorter and better performing solutions, as it is designed to maximize the discounted sum of rewards. In practice, we propose applying a step cost for each executed operation. Therefore, the structural optimization of the circuits is inherent in the design of our approach.

To achieve practical effectiveness, quantum circuits must also be designed to accommodate the constraints of existing NISQ hardware. Beyond the circuit depth, these constraints include the limited number and connectivity of qubits, the available gate set, and the high susceptibility to errors (Bharti et al., 2022). The qubit routing problem describes the challenge of mapping logical to physical qubits (Childs et al., 2019), which might not be connected due to experimental limitations. To allow arbitrarily placing two-qubit gates, such as CNOT, SWAP operations are applied to connect pairs. However, taking the resulting circuit depth into account, this constitutes an NP-hard combinatorial optimization problem (Siraichi et al., 2018). Besides popular approaches such as sorting networks (Steiger et al., 2018), or proprietary compiler-specific methods, the application of RL operating on the entire circuit has been shown to outperform state-of-the-art methods (Herbert & Sengupta, 2018; Pozzi et al., 2022). Regarding the design of high-fidelity error-tolerant gate sets, compensating for the processes that induce hardware errors on NISQ devices, Baum et al. (2021) proposed the use of RL to manipulate a small set of accessible experimental control signals. Considering the qubit routing problem as well as error mitigation, our approach does not yet take these hardware-specific properties into account, but can be easily extended to do so. To respect for reduced hardware connectivity, the action space for multi-qubit gates could be reduced to qubits that are directly connected to each other in the hardware topology. In regards to Error Mitigation, the state of the RL agent could be changed from state vectors to density matrices in order to model errors occurring, e.g., due to decoherence or imperfect gates.

Overall, those applications further underscore the efficacy of RL in quantum computing. Yet, most approaches consider RL for specific applications, using specialized discrete gate sets, where the parameters need to be optimized post hoc.

4. Quantum Circuit Design Objectives for RL

For a unified collection of RL challenges that arise from quantum architecture search and circuit optimization, we formalize generic *state preparation* and *unitary composition* objectives along with reward measures and specific target states in the following.

State Preparation (SP) SP denotes the objective of finding a sequence of operations that will generate a desired quantum state from a given initial state $|0\rangle^{\otimes \eta}$, with the number of available qubits η . Denoting the final output state as $s_t = |\Phi\rangle \in \mathbb{C}^{2^\eta}$, the generated gate sequence can be seen as the unitary mapping

$$U : |0\rangle^{\otimes \eta} \mapsto |\Phi\rangle \quad (8)$$

We measure success in this objective based on the distance between $|\Phi\rangle$ and the target state $|\Psi\rangle$ using the *fidelity* F , measuring the overlap between the two states:

$$F(\Phi, \Psi) = |\langle \Phi | \Psi \rangle|^2 \in [0, 1] \quad (9)$$

This definition intrinsically suggests a setting of sparse rewards for the SP objective, as we are not interested in the quantum state during an episode, but rather want to maximize the final fidelity. Therefore, we define the accompanying reward as follows:

$$\mathcal{R}^{SP}(s_t, a_t) = F(s_t, \Psi) \quad (10)$$

As a proof of concept, we propose using the following states:

- The *Bell state*, to reflect basic entanglement:

$$|\Phi^+\rangle \equiv \frac{|00\rangle + |11\rangle}{\sqrt{2}} \quad (11)$$

- The *Greenberger–Horne–Zeilinger state* (GHZ), to reflect entanglement of a variable number of n qubits:

$$|GHZ\rangle \equiv \frac{|0\rangle^{\otimes n} + |1\rangle^{\otimes n}}{\sqrt{2}} \quad (12)$$

- The *Haar random state*, as a benchmark for preparing an arbitrary state:

$$|\tilde{U}\rangle = \tilde{U} |0\rangle^{\otimes \eta} \quad (13)$$

However, note that further, more intricate states are easily extendable.

Unitary Composition (UC) UC denotes the objective of composing an arbitrary unitary transformation with only a finite choice of operations. UC can also be seen as a more general case of SP, in which the mapping of Eq. (8) must

not only apply to a specific input state, but to all possible inputs. Note that while the choice of operations is finite, due to including the parameter Φ into the action space, the gate set itself is arguably infinite. A necessary condition for decomposing a theoretical unitary circuit into a primitive set of operations is that this set is universal by means of [Dawson & Nielsen \(2006\)](#). The *Solovay-Kitaev theorem*, however, states that there exists a finite sequence of gates that approximate any target unitary transformation U to arbitrary accuracy, without providing such a sequence. Assuming that any circuit or sequence of gates $\Sigma_t = \langle a_0, \dots, a_t \rangle$, generated by policy π , can be represented as a unitary matrix $V(\Sigma_t) \in \mathbb{C}^{2^\eta \times 2^\eta}$, we define the distance D to the target V as:

$$D(U, V(\Sigma_t)) = \|U - V(\Sigma_t)\|^2, \quad (14)$$

with $\|\cdot\|$ denoting the Frobenius norm. As this can take on any positive real number and still reflects a loss to be minimized rather than a reward, it is necessary to map this measure to a manageable value range:

$$R^{UC}(a_t, s_t) = 1 - \arctan(D(U, V(\Sigma_t))) \quad (15)$$

As a proof of concept we use the following unitaries:

- The *Hadamard* operator H (7), creating superposition
- A random operator \tilde{U} according to [Ozols \(2009\)](#)
- The *Toffoli* operator defined as:

$$CCX_{a,b,c} = |0\rangle\langle 0| \otimes \mathbf{I} \otimes \mathbf{I} + |1\rangle\langle 1| \otimes \mathbf{C}\mathbf{X}, \quad (16)$$

Lastly, we consider *Hamiltonian simulation* (HS), which can be formalized as follows. Given the Hamiltonian \mathcal{H} of a quantum system, the solution to the Schrödinger equation yields a time evolution of the system according to $|\Psi(\tau)\rangle = \exp(-i\mathcal{H}\tau) |\Psi_0\rangle$. According to the Suzuki-Trotter formula, these dynamics can be approximately factorized with a rigorously upper-bounded error ([Lloyd, 1996](#)). Thus, a sequence Σ_t can be optimally chosen to produce

$$|\Phi\rangle = \left(\prod_t \Sigma_t \right) |\Psi\rangle, \quad (17)$$

such that $|\Phi\rangle$ is as close as possible to $|\Psi\rangle$ ([Bolens & Heyl, 2021](#)). However, it can be observed that the simulation of the time evolution of a Hamiltonian \mathcal{H} is mathematically equivalent to the UC of the unitary operator $\exp(-i\mathcal{H}\tau)$. While this fact can typically not be exploited in practice due to the required exponential computational resources in classical computing, we argue that due to their mathematical equivalence, RL should perform equally in the UC and HS objectives.

5. Quantum Circuit Designer

To use RL for learning to solve the previously proposed objectives, we define a generic *quantum circuit designer* (QCD) environment, in the following, formalized as an MDP. Fig. 1 shows a schematic rendering of the environment. To ensure maximal compatibility with various use cases and scenarios down the line, our framework only corresponds to a quantum device (simulator or real hardware), parameterized by its number of available qubits η and its maximally feasible circuit depth δ . To constantly monitor the current circuit, $\mathcal{P}(s_{t+1} | s_t, a_t)$ is implemented by a quantum simulator, which allows for efficient state vector readout.

State At each time step t , the agent observes the state s_t resulting from the current quantum circuit via the full complex vector representation of its state $s_t = |\Psi\rangle \in \mathbb{C}^{2^\eta}$. This state representation is chosen as it contains the maximal amount of information to be known about the output of the circuit. Although this information is only available in quantum simulators (on real hardware, $\mathcal{O}(2^\eta)$ many measurements would be needed), it represents a starting point for RL from which future work should extract a sufficient and efficiently obtainable subset of information. This 2^η -dimensional state representation is sufficient for the definition of an MDP-compliant environment, as operations on this state are required to be reversible. Thus, no history of states is needed and decisions can be made solely based on the current state. Note that this representation can be extended to allow for mid-circuit measurements when switching to a density matrix-based representation of the state, however, at the cost of a quadratically larger state space. Initially, all available qubits are in state $|0\rangle$.

Action Given this observation, the agent needs to choose a suitable action, consisting of three fragments: The operation Γ , the target Ω , and the parameter Φ . To provide a balanced action space, we propose using an extension of the previously defined universal gate set, giving the agent a choice between controlled or uncontrolled operations along the \mathbb{X} or \mathbb{Z} axis. Additionally, the agent can choose to perform a measurement \mathcal{M} or terminate the current episode, resulting in the following operation choice $\Gamma \in \{\mathbb{M}, \mathbb{Z}, \mathbb{X}, \mathbb{T}\}$. Operations following a measurement are discarded. Once all available qubits have been measured, the episode is terminated. Upon episode termination, all unused qubits are disregarded. Thus, the additional *terminate* action enables the optimization of compact yet effective architectures within the defined limits for available qubits η and feasible depth δ . If not terminated, an episode is truncated as soon as the maximum circuit depth δ is reached. Secondly, the agent needs to choose the target of the operation; one qubit q for applying the operation, and one control qubit c , $\Omega = \{q, c\} \in [0, \eta - 1]^2$.

For the terminate operation, the target fragment is discarded. If the operation qubit equals the control qubit, an uncontrolled operation is performed, resulting in the following set of gates $\mathbb{G} = \{\mathbf{RX}, \mathbf{CX}, \mathbf{P}, \mathbf{CP}\}$ (cf. Eqs. (3)-(6)) to be applied:

$$g(o, q, c) : \Gamma \times \Omega \mapsto \mathbb{G} = \begin{cases} \begin{cases} \mathbf{RX} & q = c \\ \mathbf{CX} & q \neq c \end{cases} & o = \mathbb{X} \\ \begin{cases} \mathbf{P} & q = c \\ \mathbf{CP} & q \neq c \end{cases} & o = \mathbb{Z} \end{cases} \quad (18)$$

In contrast to most related work we refrain from using a discrete action space with a gate set like *Clifford + T*. Instead, we aim to exploit the capabilities of RL to perform continuous control, like for robotic tasks. Thereby, parameterized gates can be optimized directly by the agent via the last action fragment $\Phi \in [-\pi, \pi]$. Otherwise, a second optimization pass would be needed to improve the placed continuous gates, which increases the overall complexity of the application. Also, using an external optimizer for parameterization does not suit our approach, as our aim is to benchmark the suitability of RL for QC. Note that for the CNOT gate \mathbf{CX} , the parameter is omitted. This helps reduce the action space and is motivated by the empirical lack of CRX gates in most circuit architectures. Overall, this results in the 4-dimensional action space $\langle o_t, q_t, c_t, \Phi_t \rangle = a_t \in \mathcal{A} = \{\Gamma \times \Omega \times \Theta\}$. Thus, following Eq. (18), the operation $U = g(o_t, q_t, c_t)(\Phi_t)$ is applied at time step t .

Reward The reward is kept 0 until the end of an episode is reached (either by truncation or termination). To incentivize the use of few operations, a step-cost \mathcal{C}_t is applied when exceeding two-thirds of the available operations σ :

$$\mathcal{C}_t = \max\left(0, \frac{3}{2\sigma} \left(t - \frac{\sigma}{3}\right)\right), \quad (19)$$

with $\sigma = \eta \cdot \delta \cdot 2$. We choose this bound to prevent prevalent solutions solely optimizing for minimal qubit and operation usage, which would cause immediately terminating the episode. To further incentivize the construction of useful circuits, we use the previously defined task reward functions \mathcal{R}^* according to Eq. (10) and Eq. (15) for the SP and UC challenges respectively, s.t.:

$$\mathcal{R} = \begin{cases} \mathcal{R}^*(s_t, a_t) - \mathcal{C}_t, & \text{if } t \text{ is terminal.} \\ 0, & \text{otherwise.} \end{cases} \quad (20)$$

However, in contrast to the overall domain, those are specific to the given problem instance or challenge, defined previously, and might be extended to address further objectives.

6. Implementation

The QCD environment is implemented based on *gymnasium* (Towers et al., 2023) and *pennylane* (Bergholm et al., 2018). All implementations are available here¹.

Environments As previously elaborated, the challenges of state preparation (SP) and unitary composition (UC) are either closely related to the others mathematically, accounted for by the environment design, or can be easily incorporated. As defined in section 4, we used states $\Psi \in \{|\Phi^+\rangle, |\tilde{U}\rangle, |GHZ\rangle\}$, with $\eta \in \{2, 2, 3\}$ and $\delta \in \{12, 12, 15\}$ respectively, for SP, and unitaries $U \in \{H, \tilde{U}, CCX\}$, with $\eta \in \{1, 2, 3\}$ and $\delta \in \{9, 12, 63\}$ respectively, for UC. As a proof-of-concept for the proposed environment architecture, we only conducted experiments for this initial set of challenges. However, note that the QCD allows for easy extension of both challenges by defining arbitrary target states and unitaries.

Action Space Regarding the implementation of the action space, the main challenge we face is the mixed nature of quantum control: While the selection of gates and qubits to be applied resembles a discrete decision problem, we argue that integrating continuous control over the parameterization of the placed gate is crucial to unveil the full potential of RL for QC. As current RL algorithms do not implement policies with mixed output spaces, we opt for a fully continuous action space and discretize the choice over the gate, qubit, and control contained. Yet, our long-term vision is to enable mixed control to optimally suit quantum control.

Baselines To provide a diverse set of state-of-the-art model-free baselines, we decided for A2C (Mnih et al., 2016), PPO (Schulman et al., 2017), TD3 (Dankwa & Zheng, 2019), and SAC (Haarnoja et al., 2018). A discretization of the proposed action space (especially the parameterization) would require $3 \cdot \eta^2 \cdot \varrho$ dimensions, with a resolution $\varrho = 4$, resulting in more than 100 dimensions of actions only for a 3-qubit challenge. We therefore omitted DQN baselines, only supporting discrete action spaces. All baselines are implemented extending Raffin et al. (2021) and use the default hyperparameters suggested in their corresponding publication. All policies are trained for 1M time steps. Additionally, we provide a *random* baseline averaged over 100 episodes of randomly chosen actions. For significance, all results are averaged over eight random seeds, reporting both the mean and the 95% confidence interval.

Metrics As a performance metric, we report the undiscounted sum of rewards, which we refer to as *Mean Return*, reflecting a combination of fulfilling the challenge at hand whilst using operations sparingly (cf. Eq. 20). To reflect

capabilities regarding circuit optimization, or the generation of optimized circuits, we furthermore provide the final number of utilized qubits (*Mean Qubits*) and the final depth of the circuit (*Mean Depth*). Note that the final depth of the circuit is affected by the scheduling of the sequence of operations generated by the policy, which is currently handled by the simulation. However, scheduling tasks have also been shown to be solvable RL objectives and could be integrated into the reward function to reduce the need for external compilation. Note that, regardless of defining constraints for the number of qubits η and the depth δ beforehand, the choice on the number of operations is made by the policy. For smoothing, all metrics are averaged over a sliding window of 100 episodes.

7. Evaluation

In the following, our aim is to demonstrate the challenges of current RL approaches inherent with QCD. First, we look at two elementary objectives: Constructing the Hadamard operation and preparing the 3-qubit GHZ state. As introduced earlier, the Hadamard operator is an integral component for exploiting superposition in QC and is therefore included in most elementary gate sets. However, as we focus on the choice of parameterized gates, it is precluded from our action space. Playing a central role in most quantum algorithms nevertheless, it is crucial for RL to reconstruct it. Reconstruction is possible via $H = P(\pi/2)RX(\pi/2)P(\pi/2)$. Connecting the Hadamard state to another or multiple qubits via one or multiple CNOTs yields the Bell and GHZ states, respectively. Both states likewise play a vital role in QC algorithms, expressing maximum entanglement of the involved qubits.

Fig. 2 shows the evaluation results. Regarding the Mean Return for the Hadamard composition, all compared algorithms exceed the random baseline. Yet, presumably due to the intricate action space, no approach reaches upper reward regions or is even capable of flawlessly reproducing the operator. Overall, PPO shows the best performance, while A2C performs worst, reaching high returns in the initial 200k time steps, but deteriorating over the subsequent steps. Looking at the Mean Qubits used reveals that most approaches converge to utilizing the qubit at hand, indicating the availability of an exploitable learning signal, even though inherently hard to explore. Here, the reason for the decrease in A2C performance can also be found, showing the tendency not to use the available qubit in the second half of training. Regarding the utilized circuit depth, all approaches show to perform at least two operations on average before terminating or measuring. SAC initially explores circuits of maximum depth, which, according to the achieved return, were not useful. However, evincing such explorative behavior may be beneficial in finding an optimal policy to

¹<https://github.com/philippaltmann/QCD>.

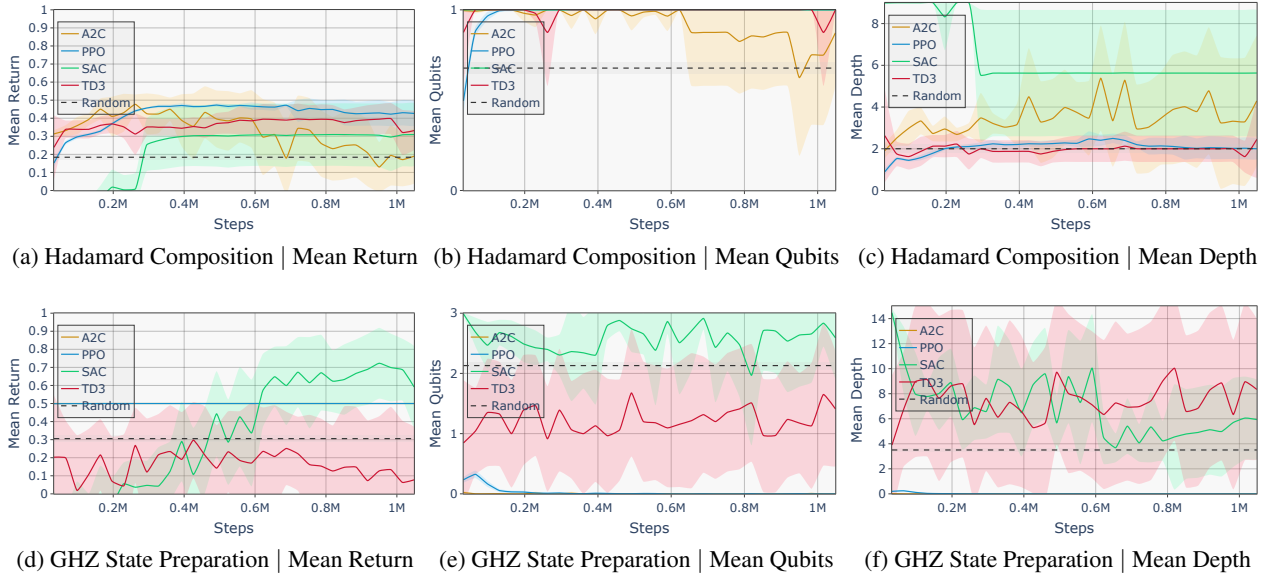


Figure 2. **Quantum Circuit Designer Evaluation:** Benchmarking A2C (orange), PPO (blue), SAC (green), and TD3 (red) for the Hadamard Composition (Fig. 2a-2c) and GHZ State Preparation (Fig. 2e-2f) challenges with regards to the Mean Return, Mean Qubits utilized, and Mean Depth of the resulting circuit, against a random baseline (dashed line). Shaded areas mark the 95% confidence intervals.

perform quantum control.

Given that the subsequent challenges of creating entanglement build upon the skill of putting qubits into superposition, which no of the compared algorithms was able to achieve, no high performances can be expected. This constitutes a further challenge that QC yields for RL: Complex circuit architectures are often built upon hierarchical building blocks. This justifies multi-level optimization approaches, resembling similar hierarchies. On the other hand, the proposed low level might yield the exploration of unconventional approaches providing out-of-the-box solutions to complex multi-level challenges.

Indications of said prospects can be observed for the GHZ state preparation results. Although not only successful for Hadamard composition, SAC reaches mean return regions above 70%. Having shown increased exploration of the circuit space previously, this seems to be a natural consequence. However, note that we look at a different challenge of state preparation here, which might be easier, as no exact resemblance of the operations is required. On the contrary, PPO and A2C yield a steady mean return of 0.5. Even though this cannot be considered a good performance, it yields improvements over the random baseline, indicating that the environment structure allows for learning reinforced behavior. Looking at both the mean number of qubits and the mean circuit depth reveals primal convergence to empty circuits, initially terminated without applying any gates. Thus, both A2C and PPO exploit a deficiency in the reward landscape, revealing a local optimum for empty circuits. Due to the

additional step cost, overcoming this local optimum would first require a performance decrease caused by the use of additional operations. TD3 on the other hand, explores various qubit and depth configurations but yields mean returns even below the random baseline. SAC, however, mostly utilizes all available qubits and explores the available depth of circuits, presumably due to the more advanced exploration mechanism for continuous control spaces.

To benchmark more advanced scenarios, Fig. 3 shows the evaluation results for random state preparation and Toffoli composition. Especially with regard to the area of quantum machine learning using variational quantum circuits, the ability to quickly put qubits into an arbitrary state is crucial to the success of the approach. The Toffoli unitary reflects an operation that cannot be directly implemented on most hardware, and therefore needs to be automatically decomposed. The increased difficulty of these challenges is reflected in the overall performance of all compared state-of-the-art approaches, merely reaching 40% of the optimal performance.

For random state preparation, SAC shows the highest return, while TD3 performs worst, merely reaching above the random baseline. Both A2C and PPO barely show any improvement throughout training, indicating inferior exploration, which is also reflected in the mean number of qubits used. The exploration problem inherent with the action space is again reflected in the mean depth of circuits, with only SAC exploring larger depths. This can be observed throughout the results and is especially notable for the Tof-

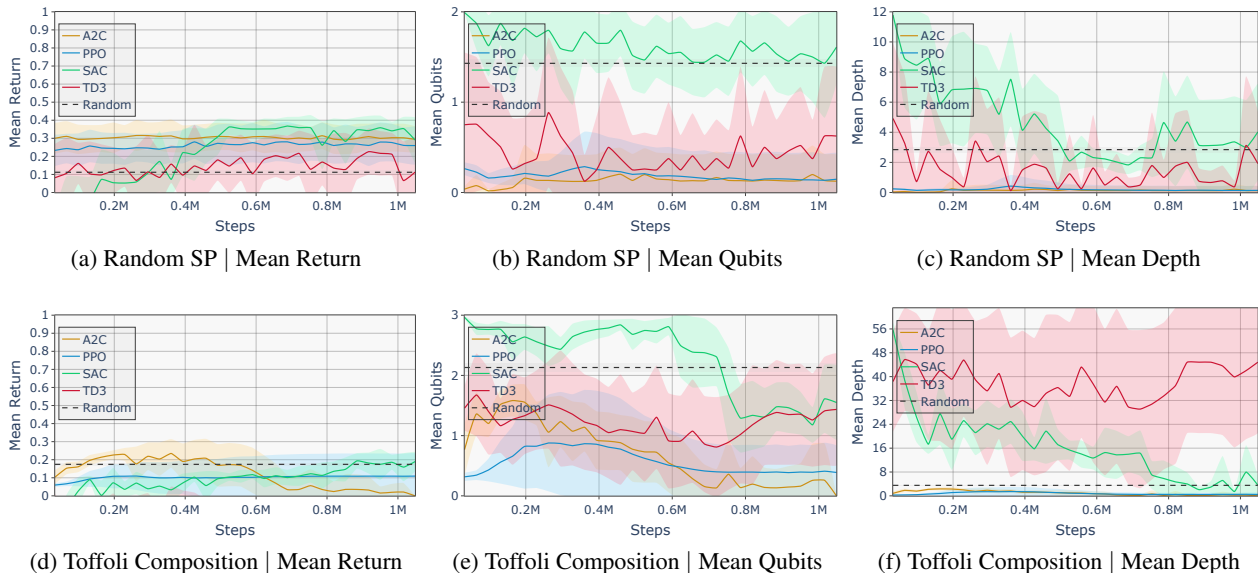


Figure 3. **Quantum Circuit Designer Evaluation:** Benchmarking A2C (orange), PPO (blue), SAC (green), and TD3 (red) for the Random State Preparation (Fig. 3a-3c) and Toffoli Composition (Fig. 3d-3f) challenges with regards to the Mean Return, Mean Qubits utilized, and Mean Depth of the resulting circuit, against a random baseline (dashed line). Shaded areas mark the 95% confidence intervals.

foli composition challenge offering depths up to 63. As expected, random unitary compositing poses an even more difficult challenge compared to random state preparation. Here, the best-performing approaches only merely exceed the mean return of the random baseline. The Toffoli composition shows even more severe complexity, with the best-performing algorithm SAC, only reaching the performance of the random baseline in the final 100k steps.

Overall, the results provide certainty that the proposed *quantum circuit designer* environment can be used to learn skills in the domain of QC using RL. Yet, current state-of-the-art approaches do not provide sufficient performance for robust and scalable applicability. Besides the chosen reward, the circuit depth and the number of used qubits have proven to be viable metrics for an in-depth analysis of the learned behavior. Across all challenges, SAC has shown to yield superior results due to its effective exploration mechanism.

8. Conclusion

We introduced the *quantum circuit designer*, a framework for benchmarking RL for the use in low-level quantum control. Furthermore, we motivated and proposed an initial set of challenges for both quantum architecture search and quantum circuit optimization, including the composition of unitary operations and the preparation of quantum states. Benchmark results for various state-of-the-art model-free RL algorithms showed the soundness of the proposed framework, as well as current challenges to be redeemed in order

for RL to be widely applicable for quantum control.

Those challenges mainly include the exploration of multimodal reward landscapes in combination with complex non-uniform high-dimensional action spaces. Considering the additional objectives, minimizing operation count and circuit depth whilst maximizing performance, separately and applying multi-objective RL concepts might improve the ability to deal with those independent goals. Furthermore, smoother reward metrics, including intermediate rewards, are needed to ease exploration of the intricate action space for quantum control. Also, the proposed state-space is currently limited by the fact that it scales exponentially with the number of qubits. For an agent to focus on relevant parts of the state-space, an attention mechanism or partial observability might be useful to further decrease the exploration challenge. In addition, simulations are currently only possible for qubit numbers of $n < 50$. Thus, approximate simulations might be useful to increase viable circuit sizes. Future work should also follow up with the collection of additional relevant states, unitaries, and Hamiltonians for SP, UC, and HS. Also, as previously mentioned, the overall objective might be extended to account for error mitigation.

Overall, however, we believe that the *quantum circuit designer* provides a profound base for future research on the application of RL to QC to build upon.

Impact Statement

By posing a generic framework for the use of reinforcement learning in quantum circuit design, alongside challenges and shortcomings of current state-of-the-art RL approaches, we aim to bridge the gap between both communities to enable interdisciplinary collaboration and ultimately advance both fields of quantum physics and machine learning research.

Acknowledgements

This work is part of the Munich Quantum Valley, which is supported by the Bavarian state government with funds from the Hightech Agenda Bayern Plus.

References

- Barenco, A., Bennett, C. H., Cleve, R., DiVincenzo, D. P., Margolus, N., Shor, P., Sleator, T., Smolin, J. A., and Weinfurter, H. Elementary gates for quantum computation. *Physical review A*, 52(5), 1995.
- Baum, Y., Amico, M., Howell, S., Hush, M., Liuzzi, M., Mundada, P., Merkh, T., Carvalho, A. R., and Biercuk, M. J. Experimental deep reinforcement learning for error-robust gate-set design on a superconducting quantum computer. *PRX Quantum*, 2(4), 2021.
- Bergholm, V., Izaac, J., Schuld, M., Gogolin, C., Ahmed, S., Ajith, V., Alam, M. S., Alonso-Linaje, G., Akash-Narayanan, B., Asadi, A., et al. Pennylane: Automatic differentiation of hybrid quantum-classical computations. *arXiv preprint arXiv:1811.04968*, 2018.
- Bharti, K., Cervera-Lierta, A., Kyaw, T. H., Haug, T., Alperin-Lea, S., Anand, A., Degroote, M., Heimonen, H., Kottmann, J. S., Menke, T., et al. Noisy intermediate-scale quantum algorithms. *Reviews of Modern Physics*, 94(1), 2022.
- Bolens, A. and Heyl, M. Reinforcement learning for digital quantum simulation. *Physical Review Letters*, 127(11), 2021.
- Bukov, M., Day, A. G., Sels, D., Weinberg, P., Polkovnikov, A., and Mehta, P. Reinforcement learning in different phases of quantum control. *Physical Review X*, 8(3), 2018.
- Childs, A. M., Schoute, E., and Unsal, C. M. Circuit transformations for quantum architectures. In *14th Conference on the Theory of Quantum Computation, Communication and Cryptography*, 2019.
- Chivilikhin, D., Samarin, A., Ulyantsev, V., Iorsh, I., Oganov, A., and Kyriienko, O. Mog-vqe: Multiobjective genetic variational quantum eigensolver. *arXiv preprint arXiv:2007.04424*, 2020.
- Colomer, L., Skotiniotis, M., and Muñoz-Tapia, R. Reinforcement learning for optimal error correction of toric codes. *Physics Letters A*, 384(17), 2020.
- Crooks, G. E. Gradients of parameterized quantum gates using the parameter-shift rule and gate decomposition. *arXiv preprint arXiv:1905.13311*, 2019.
- Dankwa, S. and Zheng, W. Twin-delayed ddpq: A deep reinforcement learning technique to model a continuous movement of an intelligent robot agent. In *Proceedings of the 3rd international conference on vision, image and signal processing*, pp. 1–5, 2019.
- Dawson, C. and Nielsen, M. The solovay-kitaev algorithm. *Quantum Information and Computation*, 6(1):81–95, January 2006. doi: 10.26421/qic6.1-6.
- Fösel, T., Niu, M. Y., Marquardt, F., and Li, L. Quantum circuit optimization with deep reinforcement learning. *arXiv preprint arXiv:2103.07585*, 2021.
- Grudzien, J., De Witt, C. A. S., and Foerster, J. Mirror learning: A unifying framework of policy optimisation. In *International Conference on Machine Learning*, pp. 7825–7844. PMLR, 2022.
- Haarnoja, T., Zhou, A., Hartikainen, K., Tucker, G., Ha, S., Tan, J., Kumar, V., Zhu, H., Gupta, A., Abbeel, P., et al. Soft actor-critic algorithms and applications. *arXiv preprint arXiv:1812.05905*, 2018.
- Harrow, A. W., Hassidim, A., and Lloyd, S. Quantum algorithm for linear systems of equations. *Physical review letters*, 103(15), 2009.
- Herbert, S. and Sengupta, A. Using reinforcement learning to find efficient qubit routing policies for deployment in near-term quantum computers, 2018.
- Kissinger, A. and van de Wetering, J. Reducing the number of non-clifford gates in quantum circuits. *Physical Review A*, 102(2), August 2020.
- Kitaev, A. Y. Quantum computations: algorithms and error correction. *Russian Mathematical Surveys*, 52(6), 1997.
- Kölle, M., Schubert, T., Altmann, P., Zorn, M., Stein, J., and Linnhoff-Popien, C. A reinforcement learning environment for directed quantum circuit synthesis. *arXiv preprint arXiv:2401.07054*, 2024.
- Kuo, E.-J., Fang, Y.-L. L., and Chen, S. Y.-C. Quantum architecture search via deep reinforcement learning. *arXiv preprint arXiv:2104.07715*, 2021.
- Lloyd, S. Universal quantum simulators. *Science*, 273(5278):1073–1078, 1996.

- Mnih, V., Kavukcuoglu, K., Silver, D., Rusu, A. A., Veness, J., Bellemare, M. G., Graves, A., Riedmiller, M., Fidjeland, A. K., Ostrovski, G., et al. Human-level control through deep reinforcement learning. *nature*, 518(7540): 529–533, 2015.
- Mnih, V., Badia, A. P., Mirza, M., Graves, A., Lillicrap, T., Harley, T., Silver, D., and Kavukcuoglu, K. Asynchronous methods for deep reinforcement learning. In *International conference on machine learning*, pp. 1928–1937. PMLR, 2016.
- Nielsen, M. A. and Chuang, I. L. *Quantum computation and quantum information*. Cambridge university press, 2010.
- Ostaszewski, M., Trenkwalder, L. M., Masarczyk, W., Scerri, E., and Dunjko, V. Reinforcement learning for optimization of variational quantum circuit architectures. *Advances in Neural Information Processing Systems*, 34: 18182–18194, 2021.
- Ozols, M. How to generate a random unitary matrix. *unpublished essay on <http://home.lu.lv/sd20008>*, 2009.
- Peruzzo, A., McClean, J., Shadbolt, P., Yung, M.-H., Zhou, X.-Q., Love, P. J., Aspuru-Guzik, A., and O’Brien, J. L. A variational eigenvalue solver on a photonic quantum processor. *Nature Communications*, 5(1), July 2014.
- Pirhooshayan, M. and Terlaky, T. Quantum circuit design search. *Quantum Machine Intelligence*, 3:1–14, 2021.
- Pozzi, M. G., Herbert, S. J., Sengupta, A., and Mullins, R. D. Using reinforcement learning to perform qubit routing in quantum compilers. *ACM Transactions on Quantum Computing*, 3(2):1–25, 2022.
- Preskill, J. Quantum computing in the nisq era and beyond. *Quantum*, 2:79, 2018.
- Puterman, M. L. *Markov decision processes: discrete stochastic dynamic programming*. John Wiley & Sons, 2014.
- Raffin, A., Hill, A., Gleave, A., Kanervisto, A., Ernestus, M., and Dormann, N. Stable-baselines3: Reliable reinforcement learning implementations. *The Journal of Machine Learning Research*, 22(1):12348–12355, 2021.
- Rattew, A. G., Hu, S., Pistoia, M., Chen, R., and Wood, S. A domain-agnostic, noise-resistant, hardware-efficient evolutionary variational quantum eigensolver. *arXiv preprint arXiv:1910.09694*, 2019.
- Schulman, J., Wolski, F., Dhariwal, P., Radford, A., and Klimov, O. Proximal policy optimization algorithms. *arXiv preprint arXiv:1707.06347*, 2017.
- Shor, P. W. Polynomial-time algorithms for prime factorization and discrete logarithms on a quantum computer. *SIAM review*, 41(2):303–332, 1999.
- Siraichi, M. Y., Santos, V. F. d., Collange, C., and Pereira, F. M. Q. Qubit allocation. In *Proceedings of the 2018 International Symposium on Code Generation and Optimization*, pp. 113–125, 2018.
- Sogabe, T., Kimura, T., Chen, C.-C., Shiba, K., Kasahara, N., Sogabe, M., and Sakamoto, K. Model-free deep recurrent q-network reinforcement learning for quantum circuit architectures design. *Quantum Reports*, 4(4):380–389, 2022.
- Steiger, D. S., Häner, T., and Troyer, M. Projectq: an open source software framework for quantum computing. *Quantum*, 2:49, 2018.
- Sutton, R. S. and Barto, A. G. *Reinforcement learning: An introduction*. MIT press, 2018.
- Towers, M., Terry, J. K., Kwiatkowski, A., Balis, J. U., de Cola, G., Deleu, T., Goulão, M., Kallinteris, A., KG, A., Krimmel, M., Perez-Vicente, R., Pierré, A., Schulhoff, S., Tai, J. J., Tan, A. J. S., and Younis, O. G. Gymnasium. 2023. URL <https://github.com/Farama-Foundation/Gymnasium>.
- van der Linde, S., de Kok, W., Bontekoe, T., and Feld, S. qgym: A gym for training and benchmarking rl-based quantum compilation. *arXiv preprint arXiv:2308.02536*, 2023.
- Watkins, C. J. and Dayan, P. Q-learning. *Machine learning*, 8:279–292, 1992.
- Zhang, S.-X., Hsieh, C.-Y., Zhang, S., and Yao, H. Differentiable quantum architecture search. *Quantum Science and Technology*, 7(4):045023, 2022.
- Zhang, Y.-H., Zheng, P.-L., Zhang, Y., and Deng, D.-L. Topological quantum compiling with reinforcement learning. *Physical Review Letters*, 125(17), 2020.